

# Lattice Model for Segmental Orientation in Deformed Polymeric Networks. 1. Contribution of Intermolecular Correlations

Burak Erman\* and Ivet Bahar

Polymer Research Center and School of Engineering, Bogazici University, Bebek, 80815 Istanbul, Turkey

Andrzej Kloczkowski and James E. Mark

Polymer Research Center and Chemistry Department, University of Cincinnati, Cincinnati, Ohio 45221

Received January 16, 1990; Revised Manuscript Received May 7, 1990

**ABSTRACT:** Intermolecular contributions to segmental orientation in uniaxially deformed amorphous networks are formulated according to a lattice model. The network chains are represented as sequences of freely jointed rodlike segments each corresponding to a Kuhn segment. The length-to-width ratio,  $x$ , of the volume occupied by a Kuhn segment varies, depending on the type of the polymeric system. For polyethylene, this ratio is estimated to be about 2. The length-to-width ratios of Kuhn segments of flexible chains may in general be taken to lie between 1 and 3. The entropy of packing of such network chains in an oriented lattice is derived, and the orientation function is evaluated as a function of extension ratio, degree of swelling, and chain stiffness. The treatment is a generalization of the original work of DiMarzio in which the reduced flexibility or the relative stiffness of chain segments was not considered. Results of calculations show that for sufficiently flexible chains, i.e., for the chains composed of Kuhn segments of nearly spherical shape, intermolecular contributions to segmental orientation are of secondary importance compared to intramolecular effects and rapidly vanish with dilution upon swelling of the network with a solvent. Intermolecular interferences to segmental orientation lead to about a 10–15% increase in the observed orientation function in dry network chains with Kuhn segments of an axial ratio  $x = 3$ .

## 1. Introduction

Segmental orientation in elastomeric networks under uniaxial deformation is traditionally expressed by the simple expression

$$S_0 = \frac{1}{5m}(\lambda^2 - \lambda^{-1}) \quad (1)$$

Here,  $S_0$  is the orientation function or the second Legendre function,  $m$  is the number of Kuhn segments in a network chain, and  $\lambda$  is the extension ratio defined as the ratio of the deformed length of a sample to that in the reference state. Equation 1, obtained first by Kuhn and Gr $\ddot{u}$ n,<sup>1</sup> represents the leading term of a more general expression based on the inverse Langevin equation.<sup>1–3</sup> The latter is derived from the fundamental assumption that the chain segments do not interact with their neighbors, i.e., intermolecular effects on segmental orientation are absent and the chains are phantomlike. Due to the phantomlike nature of the chains, the theory of Kuhn and Gr $\ddot{u}$ n is referred to in the literature as “gaslike”. The subscript zero in eq 1 indicates that this expression represents segmental orientation in a gaslike environment.

Various theoretical attempts have been made to improve the gaslike theory. The effect of intermolecular interferences has first been considered in a lattice model by DiMarzio.<sup>4</sup> This work is of fundamental importance because it is the first attempt to incorporate the idea of competition of chain segments for space in an oriented liquidlike environment. Tanaka and Allen later attempted to improve the work of DiMarzio.<sup>5</sup> Intermolecular contributions to orientation were also analyzed by Jarry and Monnerie<sup>6</sup> by a phenomenological model in which nematic interactions between neighboring segments in a liquid were postulated. Those theories<sup>4–6</sup> are referred to as “liquidlike” theories in recognition of the fact that the molecules are embedded in a lattice where a segment excludes its volume from its immediate neighbors. The

model of Tanaka and Allen leads to values of segmental orientation in the dry state, which are about 50–100% larger than those predicted by the gaslike theory. By intuitive reasoning, this rather large contribution from liquidlike sources may be expected to occur in networks with relatively stiff chains but should be much less in a medium with highly flexible chains. One thus expects segmental orientation to depend also on the degree of stiffness of the chains. The lattice models of DiMarzio and of Tanaka and Allen, being simple representations of a liquidlike medium, do not depict the role of chain stiffness on segmental orientation. The present study is an attempt to improve the liquidlike theory in this direction. For this purpose, we adopt the recent lattice theory of Flory<sup>7</sup> for chains with freely jointed rodlike segments. The length-to-width ratio of each segment of a chain, which is a measure of chain stiffness, is thus incorporated into the theory of segmental orientation.

## 2. Model and Assumptions

The network consists of  $n_2$  freely jointed chains each containing  $m$  segments, referred to as “Kuhn segments”, of length  $l$ . Each chain is attached to an active junction at its two extremities. Although the freely jointed chain is a hypothetical model, its correspondence to a real chain may be established by scaling arguments.<sup>8</sup> The number  $m_r$  and length  $l_r$  of segments in a real chain are related to  $m$  and  $l$  as

$$ml = r_{\max} = m_r l_r \cos(\theta/2) \\ ml^2 = \langle r^2 \rangle_0 = C_\infty m_r l_r^2 \quad (2)$$

where  $r_{\max}$  is the maximum stretched length of the real chain,  $\theta$  is the supplemental bond angle,  $\langle r^2 \rangle_0$  is the mean-squared end-to-end length in the unperturbed state, and  $C_\infty$  is the characteristic ratio. For polyethylene (PE), calculations lead to<sup>8</sup>  $m_r/m \approx 10$  and  $l/l_r \approx 8$ . A more rigorous analysis of the equivalent segment size of a freely

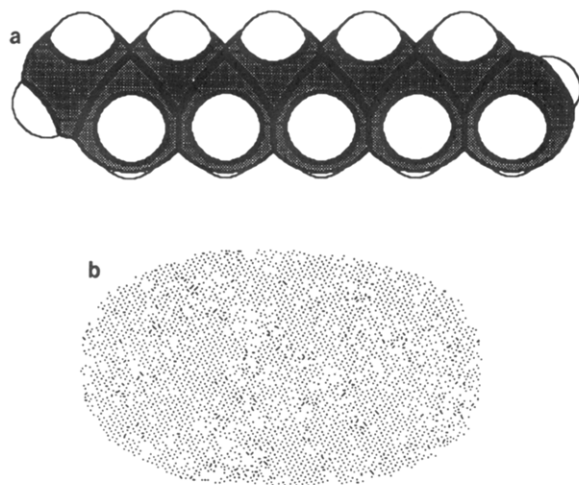


**Figure 1.** (a) Space-filling shape of a segment of 10 bonds in the all-trans form. (b) The approximate root-mean-square dimensions of the 10-bond chain.

jointed chain for PE by matching the higher order moments of the end-to-end distance of the real and the freely jointed chain leads to  $m_r/m \approx 20-22$ .<sup>9</sup> A segment of a polyethylene chain with 10–22 bonds may be viewed as a rodlike object, as is clearly demonstrated by the detailed calculations of Yoon and Flory<sup>9</sup> some years ago. The “average” shape of a polyethylene chain of 10 bonds, according to their work, may be visualized as approximately of ellipsoidal form. To estimate the corresponding length-to-width ratio or the so-called axial ratio  $x$ , the following approach may be used: from the persistence vectors along the axial and lateral directions, the mean end-to-end separation is estimated to be 6.3 Å for a PE segment of about 10 bonds. Upon consideration of the fluctuations in dimensions, both in the transverse and longitudinal directions, values of about 9.5 and 4.5 Å are found for the respective length and diameter of a representative cylindrical volume, which leads to an axial ratio of  $x \approx 2$ . The space-filling shape of a segment of 10 bonds in the all-trans form is shown in Figure 1a. The mean shape of such a segment obtained from the mean-squared dimensions given above is shown in Figure 1b. Calculations for other flexible chains lead to similar values for the length-to-width ratios. This value, although much less than these for stiffer chains such as liquid-crystal-forming molecules is nevertheless indicative of a small degree of anisotropy of a Kuhn segment. The network chains when viewed in this way conform with the Flory<sup>7</sup> model of a system of rods connected by flexible joints, each rod corresponding to a Kuhn segment.

Figure 2a displays an illustrative network chain consisting of 20 Kuhn segments (i.e., freely jointed rods) between two tetrafunctional junctions A and B. For simplicity, the network chains will be assumed to be monodisperse, i.e., composed of the same number  $m$  of rods, with all rods having an identical axial ratio  $x$ . The lateral dimensions of the rods will be of the size of solvent molecules or lattice sites. The model presented below may be readily adapted to the case of more than one lattice site occupied by either solvent molecules or the rodlike segments in the lateral direction, following an early treatment by Flory.<sup>10</sup> Let us now focus on a given segment of a network chain shown in Figure 2b. The orientation of the segment is defined by the two Euler angles,  $\Psi_k$  and  $\phi_k$ . The  $Z$  direction in the figure indicates the preferred direction, also referred to as the domain axis. In a simple extension, this direction coincides with the direction of stretch. The subscript  $k$  indicates that the orientation of the segment lies within the  $k$ th solid angle. In conformity

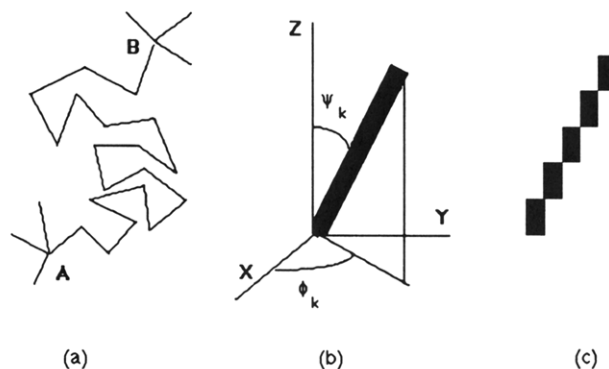


**Figure 2.** (a) Network chain of 20 Kuhn segments between the two tetrafunctional junctions A and B. (b) A segment of a chain, with  $\Psi_k$  and  $\phi_k$  representing the polar and azimuthal angles. The coordinates  $XYZ$  represent a laboratory fixed system, with  $Z$  showing the direction of stretch, or the preferred direction, in uniaxial extension. (c) Division of the segment into  $y_k = x \sin \Psi_k$  submolecules, each oriented along the preferred direction.

with the lattice treatment of Flory and collaborators,<sup>7,11,12</sup> the accommodation of the rod in the lattice is achieved through its representation by a sequence of  $y_k = x \sin \Psi_k$  submolecules, occupying each  $x/y_k$  sites and oriented along the preferred direction as shown in Figure 2c. Thus,  $y_k$  characterizes the orientation of the given rod. It is expressed in terms of  $\Psi_k$  and  $\phi_k$  as<sup>12</sup>

$$y_k = x \sin \Psi_k (|\cos \phi_k| + |\sin \phi_k|) \quad (3)$$

for the rod exhibiting that particular orientation. According to this definition, the value of  $y_k$  increases as the rod becomes disoriented. It is therefore referred to as the disorientation index.

The junctions of the network at the extremities of each chain are assumed to displace affinely with macroscopic deformation. This assumption, which is also employed by Kuhn and Gr $\ddot{u}$  n, is not exactly correct<sup>13</sup> but simplifies the problem to a large extent. Improvements in the theory by assuming nonaffine displacements of junctions may, however, be considered in a mean-field sense as has been done previously.<sup>11</sup> Additionally, the volume of the network is assumed to be constant throughout the deformation.

### 3. Exact Formulation of the Problem

**Partition Function and Free Energy of Mixing.** For a system of  $n_2$  polymer and  $n_1$  solvent molecules in a lattice consisting of  $n_0$  sites, the respective volume fractions are given by

$$\begin{aligned} v_2 &= m x n_2 / n_0 \\ v_1 &= n_1 / n_0 \end{aligned} \quad (4)$$

The expected number,  $v_{j+1}$ , of ways for adding the  $(j+1)$ th chain molecule to  $n_0$  lattice sites with  $m x j$  of them already occupied by  $j$  chain molecules is obtained according to the lattice theory of rodlike particles<sup>7</sup> as

$$v_{j+1} = (z-1)^{m-1} \frac{(n_0 - m x j)! [n_0 - m(x - \bar{y})(j+1)]!}{[n_0 - m x (j+1)]! [n_0 - m(x - \bar{y})j]!} \frac{1}{n_0^{m\bar{y}-1}} \quad (5)$$

where  $z$  is the coordination number of the lattice and the mean disorientation index,  $\bar{y}$ , is defined by

$$\bar{y} = \frac{1}{n_2 m} \sum_{l=1}^{n_2} \sum_k n_{l,k} y_k \quad (6)$$

Here,  $n_{l,k}$  indicates the number of segments of the  $l$ th chain,

whose orientation lies within the  $k$ th solid angle, and  $y_k$  is the corresponding disorientation index. The index  $k$  in the last summation denotes all sets of solid angles available to the rods.

The computation of  $\nu_{j+1}$  enables us to calculate the combinatorial part  $Z_{\text{comb}}$  of the partition function for the lattice from

$$Z_{\text{comb}} = \left( \prod_{j=1}^{n_2} \nu_j \right) / n_2! \quad (7)$$

The orientational part of the partition function is

$$Z_{\text{orient}} = \prod_{j=1}^{n_2} m! \prod_k \frac{\omega_k^{n_{j,k}}}{n_{j,k}!} \quad (8)$$

Here,  $\omega_k$  is the  $k$ th fractional range of solid angle. The total configuration partition function of the mixture is found from

$$Z_m = Z_{\text{comb}} Z_{\text{orient}} \quad (9)$$

The latter is used in evaluating the Helmholtz free energy change of mixing according to

$$\Delta A_m = -k_B T \ln Z_m \quad (10)$$

where  $k_B$  is the Boltzmann constant and  $T$  is the absolute temperature. When the Stirling approximation is used for factorials,  $-\ln Z_{\text{comb}}$  may be written as

$$-\ln Z_{\text{comb}} = n_1 \ln \nu_1 + n_2 \ln (\nu_2 / mx) - (n_1 + n_2 m \bar{y}) \ln [1 - \nu_2 (1 - \bar{y} / x)] + n_2 (m \bar{y} - 1) - n_2 (m - 1) \ln (z - 1) \quad (11)$$

and  $-\ln Z_{\text{orient}}$  is simplified as

$$-\ln Z_{\text{orient}} = \sum_{j=1}^{n_2} \sum_k n_{j,k} \ln \frac{n_{j,k}}{\omega_k m} \quad (12)$$

Equations 11 and 12 are readily substituted into eqs 9 and 10 to obtain the free energy change of mixing.

**Oriental Distribution under Deformation.** If there are no constraints imposed on the system, then an equilibrium distribution of rods among different orientations is obtained by minimizing the free energy of the system with respect to  $n_{j,k}$ . The imposition of external constraints requires the use of Lagrange multipliers while minimizing the free energy.<sup>2</sup> We fix the end-to-end vectors for each of the  $n_2$  chain molecules. Thus

$$\frac{r_{Zj}}{l} = \sum_k n_{j,k} \cos \Psi_k \quad (13)$$

$$\frac{r_{Xj}}{l} = \sum_k n_{j,k} \sin \Psi_k \cos \phi_k \quad (14)$$

$$\frac{r_{Yj}}{l} = \sum_k n_{j,k} \sin \Psi_k \sin \phi_k \quad (15)$$

Here,  $r_{Xj}$ ,  $r_{Yj}$ , and  $r_{Zj}$  denote  $X$ ,  $Y$ , and  $Z$  components of the end-to-end vector  $\mathbf{r}$  for the  $j$ th molecule, and  $l$  is the length of a rod. It should be noted that the constraints given by eqs 13–15, where each Cartesian component of the end-to-end vector is kept fixed, are different from that of the Kuhn and Gr $\ddot{u}$  n treatment. In the latter, only the component along the direction of stretch is fixed. The distribution of  $n_{j,k}$  is additionally subject to the constraint

$$m = \sum_k n_{j,k} \quad (16)$$

The equilibrium distribution of rods between different orientations with constraints given by eqs 13–16 is determined by the equation

$$\frac{\partial}{\partial n_{j,k}} [\ln Z_{\text{comb}} + \ln Z_{\text{orient}} + \alpha \sum_{k'} n_{j,k'} + \beta \sum_{k'} n_{j,k'} \cos \Psi_{k'} + \gamma \sum_{k'} n_{j,k'} \sin \Psi_{k'} \cos \phi_{k'} + \delta \sum_{k'} n_{j,k'} \sin \Psi_{k'} \sin \phi_{k'}]_{n_1, n_2, n_{j,k'}} = 0 \quad (17)$$

Here,  $\alpha$ ,  $\beta$ ,  $\gamma$ , and  $\delta$  are Lagrange multipliers and the summations are performed over all orientations  $k'$  different from  $k$ . Substituting  $-\ln Z_{\text{comb}}$  and  $-\ln Z_{\text{orient}}$  given by eqs 11 and 12 and performing the above differentiation, we obtain

$$\frac{n_{j,k}}{m} = \omega_k \exp[-a y_k + \alpha - 1 + \beta \cos \Psi_k + \gamma \sin \Psi_k \cos \phi_k + \delta \sin \Psi_k \sin \phi_k] \quad (18)$$

where

$$a = -\ln [1 - \nu_2 (1 - \bar{y} / x)] \quad (19)$$

It should be noted that  $Z_{\text{comb}}$  depends implicitly on  $n_{j,k}$  through  $\bar{y}$ , and the partial derivative  $\partial \bar{y} / \partial n_{j,k} = y_k / n_2 m$  has been used in deriving eq 18. This relies on the reasonable approximation that the distribution of orientations in a given rod is equated to that of the whole ensemble. This approximation becomes rigorous when the network chain is sufficiently long. Equation 18 reflects the probability distribution of different orientations among the rods composing the  $j$ th chain. It results from two effects: (i) orientation due to stretching of the chain from its two ends, i.e., orientation of the network chain in the gaslike medium, and (ii) orientation resulting from intermolecular correlations or from local exclusion of the volume of one segment to its neighbors. The latter effect enters eq 18 through the  $(a y_k)$  term in the exponent. In the absence of intermolecular correlations, the difference between  $\bar{y}$  and  $x$  introduced by the lattice model vanishes. Equating  $\bar{y} / x$  to unity in eq 19 leads to  $a = 0$ . The distribution given by eq 18 then reduces to

$$\frac{n_{j,k;\text{isotropic}}}{m} = \frac{\sin \Psi_k d\Psi_k d\phi_k}{4\pi} \exp(\alpha') \exp[\beta \cos \Psi_k + \gamma \sin \Psi_k \cos \phi_k + \delta \sin \Psi_k \sin \phi_k] \quad (20)$$

where the solid angle  $\omega_k$  in eq 18 has been replaced by  $(1/4\pi) \sin \Psi_k d\Psi_k d\phi_k$ , and  $\alpha - 1$  in eq 18 has been replaced by  $\alpha'$ . Correspondence to the Kuhn and Gr $\ddot{u}$  n result is obtained by equating  $\gamma$  and  $\delta$  in eq 20 to zero.

The Lagrange multipliers  $\alpha$ ,  $\beta$ ,  $\gamma$ , and  $\delta$  are to be determined from eqs 13–16. When eq 18 is used and summations over directions are replaced by integrals, the conditions imposed by the constraints may be written as

$$1 = \frac{1}{4\pi} \int_0^{2\pi} d\phi_k \int_0^\pi d\Psi_k \sin \Psi_k \exp\{-a y_k - 1 + \alpha + \beta \cos \Psi_k + \gamma \sin \Psi_k \cos \phi_k + \delta \sin \Psi_k \sin \phi_k\} \quad (21)$$

$$\frac{r_{Zj}}{ml} = \frac{1}{4\pi} \int_0^{2\pi} d\phi_k \int_0^\pi d\Psi_k \sin \Psi_k \cos \Psi_k \exp\{-a y_k - 1 + \alpha + \beta \cos \Psi_k + \gamma \sin \Psi_k \cos \phi_k + \delta \sin \Psi_k \sin \phi_k\} \quad (22)$$

$$\frac{r_{Xj}}{ml} = \frac{1}{4\pi} \int_0^{2\pi} d\phi_k \int_0^\pi d\Psi_k \sin^2 \Psi_k \cos \phi_k \exp\{-a y_k - 1 + \alpha + \beta \cos \Psi_k + \gamma \sin \Psi_k \cos \phi_k + \delta \sin \Psi_k \sin \phi_k\} \quad (23)$$

$$\frac{r_{Yj}}{ml} = \frac{1}{4\pi} \int_0^{2\pi} d\phi_k \int_0^\pi d\Psi_k \sin^2 \Psi_k \sin \phi_k \exp\{-a y_k - 1 + \alpha + \beta \cos \Psi_k + \gamma \sin \Psi_k \cos \phi_k + \delta \sin \Psi_k \sin \phi_k\} \quad (24)$$

It is noted that the Lagrange multiplier  $\alpha$  may be eliminated from eqs 22–24 by dividing each of them by eq 21. A further simplification will be the following: Equations 22–24 are independently satisfied by each of the  $n_2$  network chains. Considering the ensemble average of all the network chains, we will approximate  $r_{Xj}$ ,  $r_{Yj}$ , and  $r_{Zj}$  in the following development by their root-mean-square values; i.e.

$$\begin{aligned} r_{Zj} &= \langle r_Z^2 \rangle^{1/2} \\ r_{Xj} &= \langle r_X^2 \rangle^{1/2} \\ r_{Yj} &= \langle r_Y^2 \rangle^{1/2} \end{aligned} \quad (25)$$

Under these approximations the subscripts  $j$  in eqs 22–24 may be omitted.

For freely jointed chains under affine deformation the mean-square components of  $\mathbf{r}$  are related to those in the free state by

$$\begin{aligned} \langle r_Z^2 \rangle &= \lambda_Z^2 \langle r_Z^2 \rangle_0 = \lambda_Z^2 m l^2 / 3 \\ \langle r_X^2 \rangle &= \lambda_X^2 \langle r_X^2 \rangle_0 = \lambda_X^2 m l^2 / 3 \\ \langle r_Y^2 \rangle &= \lambda_Y^2 \langle r_Y^2 \rangle_0 = \lambda_Y^2 m l^2 / 3 \end{aligned} \quad (26)$$

Here  $\langle r_i^2 \rangle_0$  is the mean-square  $i$ th component of  $\mathbf{r}$  prior to deformation, and  $\lambda_i$  is the extension ratio along the direction  $i$  defined as the ratio of the final length to the reference length. For uniaxial deformation

$$\begin{aligned} \lambda_Z &= \lambda \\ \lambda_X &= \lambda_Y = 1/(\lambda v_2)^{1/2} \end{aligned} \quad (27)$$

Substitution from eq 27 into eq 26 leads to

$$\langle r_Z^2 \rangle^{1/2} / l = \lambda (m/3)^{1/2} \quad (28)$$

$$\langle r_X^2 \rangle^{1/2} / l = \langle r_Y^2 \rangle^{1/2} / l = (m/3\lambda v_2)^{1/2} \quad (29)$$

Also the Lagrange multipliers  $\gamma$  and  $\delta$  are equal to each other for uniaxial deformation. In this particular case, by combining eqs 28 and 29 with eqs 21–25, we obtain

$$\frac{\lambda}{(3m)^{1/2}} = \frac{\int_0^{2\pi} d\phi \int_0^\pi d\Psi \cos \Psi f(\phi, \Psi)}{\int_0^{2\pi} d\phi \int_0^\pi d\Psi f(\phi, \Psi)} \quad (30)$$

and

$$\frac{1}{(3m\lambda v_2)^{1/2}} = \frac{\int_0^{2\pi} d\phi \int_0^\pi d\Psi \sin \Psi \cos \phi f(\phi, \Psi)}{\int_0^{2\pi} d\phi \int_0^\pi d\Psi f(\phi, \Psi)} \quad (31)$$

where  $f(\phi, \Psi)$  is the orientational distribution function given by

$$f(\phi, \Psi) = \sin \Psi \exp[-a x \sin \Psi (|\cos \phi| + |\sin \phi| + \beta \cos \Psi + \gamma \sin \Psi (\cos \phi + \sin \phi))] \quad (32)$$

The dummy subscript  $k$  is omitted in writing eqs 30 and 31. These two equations additionally require the knowledge of  $\bar{y}$  since the latter is contained through  $a$  as defined by eq 19. Equations 18 and 3 lead to

$$\frac{\bar{y}}{x} = \frac{\int_0^{2\pi} d\phi \int_0^\pi d\Psi \sin \Psi (|\cos \phi| + |\sin \phi|) f(\phi, \Psi)}{\int_0^{2\pi} d\phi \int_0^\pi d\Psi f(\phi, \Psi)} \quad (33)$$

It should be noted that eq 33 for  $\beta = \gamma = 0$  differs from

the corresponding equation in the Flory–Ronca paper<sup>12</sup> because the problem was simplified in the latter by preaveraging  $\gamma$  over the angle  $\phi$ , which reduces the double integration to single integration over  $\Psi$  only. Exact calculations performed recently<sup>14</sup> show that the approximation introduced by preaveraging does not lead to significant differences. However, to keep generality, this approximation will not be adopted in the present work.

Equations 30, 31, and 33 form a system of three nonlinear equations to be solved simultaneously for  $\bar{y}$ ,  $\beta$ , and  $\gamma$ , which are all functions of  $\lambda$ . The evaluation of  $\bar{y}$ ,  $\beta$ , and  $\gamma$  enables us to calculate other quantities of interest such as

$$\langle \cos \Psi \rangle = \frac{1}{m} \sum_{i=1}^m \cos \Psi_i = \frac{1}{m} \sum_k n_{j,k} \cos \Psi_k = \frac{\lambda}{(3m)^{1/2}} \quad (34)$$

and

$$\langle \cos^2 \Psi \rangle = \frac{\int_0^{2\pi} d\phi \int_0^\pi d\Psi \cos^2 \Psi f(\phi, \Psi)}{\int_0^{2\pi} d\phi \int_0^\pi d\Psi f(\phi, \Psi)} \quad (35)$$

which is used in the evaluation of the orientation function  $S = 3 \langle \cos^2 \Psi \rangle / 2 - 1/2$ .

#### 4. An Approximate Closed-Form Solution

Equations 30, 31, and 33 may be solved analytically for small  $\beta$ ,  $\gamma$ , and small  $a$ , i.e., small  $(\bar{y}/x - 1)$ , by expanding the trigonometric functions in the exponential part of eq 32 into the Taylor series and keeping only the terms that are linear in  $a$ ,  $\beta$ , and  $\gamma$ . The resulting simpler equations are readily integrated to yield

$$\frac{\lambda}{(3m)^{1/2}} = \frac{\int_0^{2\pi} d\phi \int_0^\pi d\Psi \cos \Psi g(\phi, \Psi)}{\int_0^{2\pi} d\phi \int_0^\pi d\Psi g(\phi, \Psi)} = \frac{\beta/3}{1 - ax} \quad (36)$$

$$\frac{1}{(3m\lambda v_2)^{1/2}} = \frac{\int_0^{2\pi} d\phi \int_0^\pi d\Psi \sin \Psi \cos \phi g(\phi, \Psi)}{\int_0^{2\pi} d\phi \int_0^\pi d\Psi g(\phi, \Psi)} = \frac{\gamma/3}{1 - ax} \quad (37)$$

where

$$g(\phi, \Psi) = \sin \Psi - ax \sin^2 \Psi [|\cos \phi| + |\sin \phi| + \beta \cos \Psi \sin \Psi + \gamma \sin^2 \Psi (\cos \phi + \sin \phi)] \quad (38)$$

In the first approximation

$$\beta = (3/m)^{1/2} \lambda (1 - ax) \approx (3/m)^{1/2} \lambda \quad (39)$$

$$\gamma = (3/m\lambda v_2)^{1/2} (1 - ax) \approx (3/m\lambda v_2)^{1/2} \quad (40)$$

To calculate  $\bar{y}/x$ , we expand both the numerator and the denominator in eq 33 up to the second order in  $a$ ,  $\beta$ , and  $\gamma$  and obtain

$$\frac{\bar{y}}{x} = \frac{1 - \frac{2}{3}ax\left(1 + \frac{2}{\pi}\right) + \frac{5}{8}a^2x^2 + \frac{1}{8}\beta^2 + \frac{3}{8}\gamma^2}{1 - ax + \frac{1}{3}a^2x^2\left(1 + \frac{2}{\pi}\right) + \frac{1}{6}\beta^2 + \frac{1}{3}\gamma^2} \approx 1 - \frac{ax}{3}\left(\frac{4}{\pi} - 1\right) - \frac{1}{24}(\beta^2 - \gamma^2) \quad (41)$$

with the lowest order terms in  $a$ ,  $\beta$ , and  $\gamma$  kept only after division. Using the approximation

$$a = -\ln[1 - v_2(1 - \bar{y}/x)] \approx v_2(1 - \bar{y}/x) \quad (42)$$

in eq 41, we obtain

$$a = \frac{\frac{v_2}{24}(\beta^2 - \gamma^2)}{\left[1 - \frac{xv_2}{3}\left(\frac{4}{\pi} - 1\right)\right]} = \frac{\frac{v_2}{24}(\beta^2 - \gamma^2)}{1 - \frac{x}{x_a}v_2} \quad (43)$$

with

$$x_a = \frac{3}{(4/\pi) - 1} = 10.98 \quad (44)$$

We see that  $a$  is of the order of  $\gamma^2$  and  $\beta^2$ ; i.e., terms of the order of  $a^2$  may safely be neglected in the expansions. It is interesting to note that  $x_a$  is the length-to-width ratio of segments above which the system is totally anisotropic (see the following paper for a detailed discussion). The corresponding value in the Flory-Ronca model with preaveraging  $y_k$  over  $\phi_k$  is different, namely

$$x_{a,FR} = \frac{1}{(32/3\pi^2) - 1} = 12.38 \quad (45)$$

Substituting the expressions 39 and 40 for  $\beta$  and  $\gamma$  into eq 43, we obtain

$$a = \left[ \frac{5v_2/8}{1 - (xv_2/x_a)} \right] \frac{1}{5m} \left( \lambda^2 - \frac{1}{\lambda v_2} \right) \quad (46)$$

In order to calculate  $\langle \cos^2 \Psi \rangle$ , we expand the numerator and the denominator in eq 35 up to the first order in  $a$  and the second order in  $\beta$  and  $\gamma$  and obtain

$$\langle \cos^2 \Psi \rangle = \frac{\frac{1}{3} - \frac{1}{4}ax + \frac{1}{10}\beta^2 + \frac{1}{15}\gamma^2}{1 - ax + \frac{1}{6}\beta^2 + \frac{1}{3}\gamma^2} \approx \frac{1}{3} + \frac{1}{12}ax + \frac{2}{45}(\beta^2 - \gamma^2) \quad (47)$$

The orientation function

$$S = \frac{3}{2} \langle \cos^2 \Psi \rangle - \frac{1}{2} \quad (48)$$

is obtained by substituting from eq 47 and using eq 46 for  $a$  as

$$S = \frac{1}{5m} \left( \lambda^2 - \frac{1}{\lambda v_2} \right) \left[ 1 + \frac{5x_a}{64} \frac{xv_2/x_a}{1 - (xv_2/x_a)} \right] = S_0 + S_i \quad (49)$$

where

$$S_i \equiv S_0 \left[ \frac{5x_a}{64} \frac{xv_2/x_a}{1 - (xv_2/x_a)} \right] \quad (50)$$

denotes the intermolecular contribution to segmental orientation arising from competition for space of segments in an oriented environment.

From eq 50 we see that  $S_i$  vanishes for  $x/x_a \ll 1$ . In this case, the problem reduces to orientation in a gaslike environment.  $S_i$  also decreases with increasing solvent content and equates to zero in the limiting case of  $v_2 = 0$ , as is readily seen from eq 50.

## 5. Results of Calculations and Discussion

Results of calculations for the orientation function for a dry network with  $m = 20$  are presented in Figure 3 as a function of  $\lambda$  for  $x = 1$  and 3 as identified by the lower and upper solid curves, respectively. The choice of  $m = 20$  corresponds to a network chain of about 200–400 bonds and represents a moderately cross-linked network. The

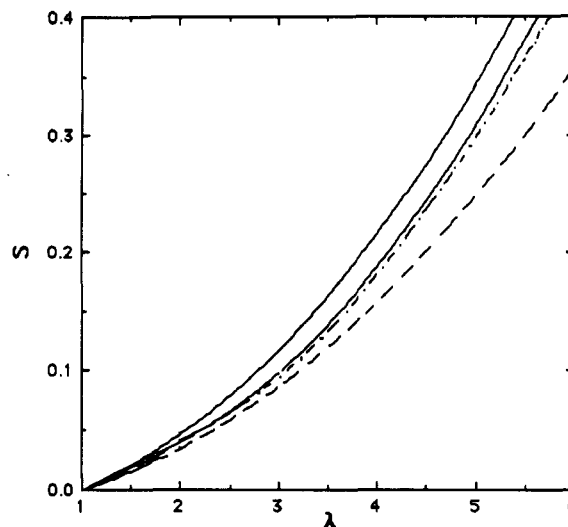


**Figure 3.** Orientation function for a dry network with  $m = 20$  presented as a function of  $\lambda$ . Solid curves are for the exact solution from eqs 30, 31, and 33 with  $x = 1$  (lower curve) and  $x = 3$  (upper curve). The dot-dashed curve is for a freely jointed chain in a gaslike environment. The dashed curve is from the simplified expression given by eq 1.

curves are obtained by solving the three nonlinear equations (eqs 30, 31, and 33) numerically. The dot-dashed curve represents segmental orientation in a freely jointed chain with 20 Kuhn segments in a gaslike environment. It is obtained by letting  $a = 0$  in eqs 30 and 31 and solving for  $\beta$  and  $\gamma$  and solving for  $\langle \cos^2 \Psi \rangle$  from eq 35 with  $a$  again set equal to zero. These results are in agreement with those obtained by Walasek,<sup>15</sup> by similar arguments on the use of constraints. The dashed curve is obtained from eq 1 and corresponds to the simplified expression for segmental orientation  $S_0$  in a gaslike environment. This curve, which is obtained for a reasonable chain length with  $m = 20$ , represents the first term of the complete solution indicated by the lowest solid curve in the figure. It leads to values significantly lower than the complete solution. The dot-dashed curve and the one for  $x = 1$  are remarkably close to each other for a very wide range of  $\lambda$  values. The upper curve in the same figure corresponding to  $x = 3$  does not lead to much larger values of segmental orientation than those shown by the dot-dashed curve and the one for  $x = 1$ . For  $\lambda = 5$ , for example,  $S$  for  $x = 3$  is only 14% larger than that shown by the dot-dashed curve. These observations lead to the conclusion that intermolecular contributions are not significant for flexible chains with  $x \leq 3$ . This is in marked contrast with results of Tanaka and Allen.<sup>5</sup>

Values of  $S$  obtained from the exact solution from eqs 30, 31, and 33 and those obtained from the linearized expression, eq 49, are compared in Figure 4 for  $x = 3$ . The difference between the two results is remarkably small for the range of  $\lambda$  shown. Their difference is even less significant for  $x = 1$ . We can thus conclude that the very simple expression for segmental orientation given by eq 49 may safely be used instead of the exact solution provided that the length-to-width ratio on the Kuhn segments is confined to relatively small values. It should be noted, however, that agreement is not possible for larger values of  $x$ , as is discussed in the following paper.<sup>16</sup>

The effect of swelling on segmental orientation is shown in Figure 5. The ordinate values are obtained as the ratio of  $S$  in a liquidlike network obtained from eq 49 to that for a gaslike network obtained from eq 1. Calculations are performed for  $\alpha = 2$ , where  $\alpha$  is the elongation relative to

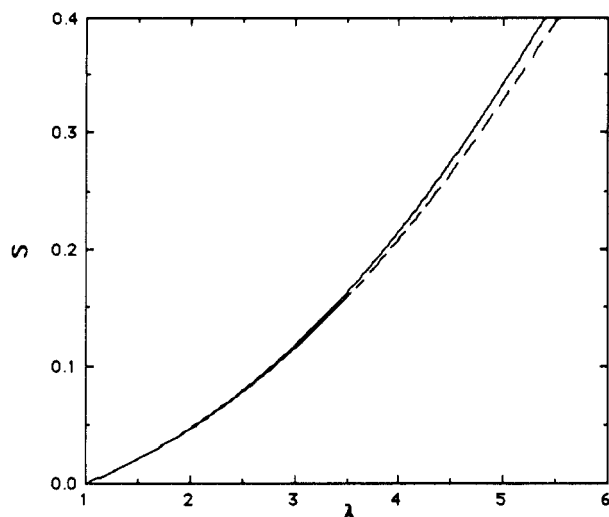


Figure 4. Comparison of values of  $S$  from the exact solution and the linearized expression, eq 49 for  $x = 3$ .

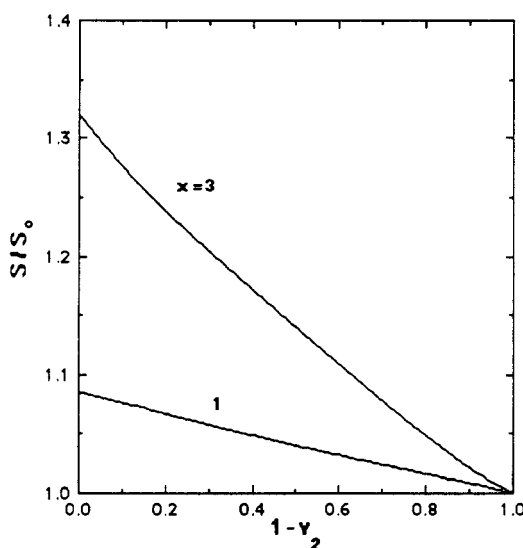


Figure 5. Dependence of  $S$  on  $v_2$  for  $x = 1$  and  $3$ . Calculations are for an extension ratio  $\alpha$  of  $2$ . The ordinate represents the ratio of  $S$  from eq 49 to that from eq 1.

the isotropic swollen sample, i.e.,  $\alpha = \lambda v_2^{1/3}$ . The abscissa represents the amount of solvent in the network. The difference between segmental orientation in the liquidlike and the gaslike networks is seen to diminish rapidly with swelling. Again, the contribution from intermolecular sources is significantly less than that obtained from the theory of Tanaka and Allen.<sup>5</sup> The solution of the swelling problem according to the exact treatment leads

to similar results for  $v_2 \geq 0.1$  and therefore is not presented separately. For values of  $v_2 \leq 0.1$  the exact solution diverges because of the finite extensibility of the chains.

The phenomenological result proposed by Jarry and Monnerie<sup>6</sup> and the analytical expression given by eq 49 are of the same functional form. Approximating  $5x_a/64$  by unity in the latter and comparing with the expression given for segmental orientation by Jarry and Monnerie shows that the parameter  $V$  of their theory may be identified with  $xv_2/x_a$  of the present treatment. However, this identification is only apparent, due to the fact that the basis of the interactions in the Jarry–Monnerie theory is energetic in nature, whereas here  $xv_2/x_a$  is obtained by considering the liquidlike nature of Kuhn segments and hence is of entropic origin. A more appropriate comparison is possible upon consideration of intermolecular thermotropic interactions.

The present treatment is confined to the study of intermolecular contributions in networks with flexible chains. The analysis of the problem for networks with stiffer chains and with possible thermotropic effects between segments resulting in phase transitions due to orientation upon stretching is considered in the following paper.<sup>16</sup>

**Acknowledgment.** It is a pleasure to acknowledge the financial support provided by the National Science Foundation through Grants DMR 84-15082 (Polymers Program, Division of Materials Research) and INT-8903327 (Sciences in Developing Countries Program).

## References and Notes

- (1) Kuhn, W.; Gr $\ddot{u}$ n, F. *Kolloid-Z.* **1942**, *101*, 248.
- (2) Volkenstein, M. *Configurational Statistics of Polymer Chains*; Timasheff, S. N., Timasheff, M. J., Eds. (translated from the Russian edition), Interscience: New York, 1963.
- (3) Treloar, L. R. G. *The Physics of Rubber Elasticity*; Clarendon Press: Oxford, England, 1975.
- (4) DiMarzio, E. A. *J. Chem. Phys.* **1962**, *36*, 1563.
- (5) Tanaka, T.; Allen, G. *Macromolecules* **1977**, *10*, 426.
- (6) Jarry, J. P.; Monnerie, L. *Macromolecules* **1979**, *12*, 316.
- (7) Flory, P. J. *Macromolecules* **1978**, *11*, 1141.
- (8) Flory, P. J. *Statistical Mechanics of Chain Molecules*; Interscience: New York, 1969. Reprinted by Hanser Publishers, Oxford University Press, 1989.
- (9) Yoon, D. Y.; Flory, P. J. *J. Chem. Phys.* **1974**, *61*, 5366.
- (10) Flory, P. J. *J. Chem. Phys.* **1941**, *9*, 660.
- (11) Flory, P. J. *Proc. R. Soc. London, A* **1954**, *234*, 73.
- (12) Flory, P. J.; Ronca, G. *Mol. Cryst. Liq. Cryst.* **1979**, *54*, 289, 311.
- (13) Mark, J. E.; Erman, B. *Rubberlike Elasticity. A Molecular Primer*; Wiley-Interscience: New York, 1988.
- (14) Kloczkowski, A.; Mark, J. E.; Erman, B. *Macromolecules* **1990**, *23*, 5035.
- (15) Walasek, J. *J. Polym. Sci., Part B: Polym. Phys.* **1988**, *26*, 1907.
- (16) Bahar, I.; Erman, B.; Kloczkowski, A.; Mark, J. E., following paper in this issue.